

Average up/down, strange, and charm quark masses with $N_f = 2$ twisted-mass lattice QCDB. Blossier,¹ P. Dimopoulos,² R. Frezzotti,³ V. Lubicz,^{4,5} M. Petschlies,⁶ F. Sanfilippo,^{2,7} S. Simula,⁵ and C. Tarantino^{4,5}¹*Laboratoire de Physique Théorique (Bâtiment 210), Université de Paris XI, Centre d'Orsay, 91405 Orsay-Cedex, France*²*Dipartimento di Fisica, Università di Roma "Sapienza", I-00185 Roma, Italy*³*Dipartimento di Fisica, Università di Roma Tor Vergata and INFN, Sezione di Roma Tor Vergata, Via della Ricerca Scientifica, I-00133 Roma, Italy*⁴*Dipartimento di Fisica, Università Roma Tre, Via della Vasca Navale 84, I-00146 Roma, Italy*⁵*INFN, Sezione di Roma Tre, Via della Vasca Navale 84, I-00146 Roma, Italy*⁶*Institut für Elementarteilchenphysik, Fachbereich Physik, Humboldt Universität zu Berlin, D-12489, Berlin, Germany*⁷*INFN, Sezione di Roma, I-00185 Roma, Italy*

(Received 25 October 2010; published 28 December 2010)

We present a high precision lattice calculation of the average up/down, strange, and charm quark masses performed with $N_f = 2$ twisted-mass Wilson fermions. The analysis includes data at four values of the lattice spacing and pion masses as low as $\simeq 270$ MeV, allowing for accurate continuum limit and chiral extrapolation. The strange and charm masses are extracted by using several methods, based on different observables: the kaon and the η_s meson for the strange quark and the D , D_s , and η_c mesons for the charm. The quark mass renormalization is carried out nonperturbatively using the regularization independent momentum-subtraction renormalization (RI-MOM) method. The results for the quark masses in the modified minimal subtraction ($\overline{\text{MS}}$) scheme read: $\bar{m}_{ud}(2 \text{ GeV}) = 3.6(2) \text{ MeV}$, $\bar{m}_s(2 \text{ GeV}) = 95(6) \text{ MeV}$, and $\bar{m}_c(\bar{m}_c) = 1.28(4) \text{ GeV}$. We also obtain the ratios $m_s/m_{ud} = 27.3(9)$ and $m_c/m_s = 12.0(3)$.

DOI: 10.1103/PhysRevD.82.114513

PACS numbers: 12.38.Gc

I. INTRODUCTION

A precise knowledge of the values of the quark masses is of great importance for testing the standard model of particle physics. From a phenomenological point of view, several useful observables to constrain the standard model or to search for new physics depend on quark masses, thus requiring accurate quark mass values in order to allow for significant theory/experiment comparisons. From a more theoretical side, explaining the quark mass hierarchy, which is not predicted by the standard model, is a deep issue and a great challenge. Lattice QCD calculations play a primary role in the determination of quark masses. Recently, the progress achieved thanks to several high statistics unquenched simulations is leading to a significant reduction of the uncertainty on the quark mass values [1–6].

In this article we present an accurate determination of the average up/down, strange, and charm quark masses performed by the European Twisted-Mass Collaboration (ETMC) with $N_f = 2$ maximally twisted-mass Wilson fermions. The high precision of this analysis is mainly due to the extrapolation of the lattice results to the continuum limit, based on data at four values of the lattice spacing, to the well controlled chiral extrapolation, which uses simulated pion masses down to $M_\pi \simeq 270$ MeV, and to the use of the nonperturbative renormalization constants calculated in [7]. The only systematic uncertainty which is not accounted for by our results is the one stemming from the missing strange and charm quark vacuum polarization effects. Those are not accessible to us with $N_f = 2$ flavor simulations. However, a comparison of $N_f = 2$ results for

the up/down and strange quark masses to already existing results from $N_f = 2 + 1$ quark flavor simulations [8] indicates that, for these observables, the error due to the partial quenching of the strange quark is smaller at present than other systematic uncertainties. The same conclusion is expected to be valid for the effects of the strange and charm partial quenching in the determination of the charm quark mass.

In this work, the calculation of the isospin averaged up/down quark mass, based on the study of the pion mass and decay constant, closely follows the strategy of [9]. At variance with the latter, however, in the present analysis we include data at four values of the lattice spacing, and use the same lattice setup for all quark mass analyses.

For the strange quark mass, the main improvement with respect to our previous work [10], which used data at a single lattice spacing only, is the continuum limit. Moreover, the chiral extrapolation is performed by using either SU(2)- or SU(3)-chiral perturbation theory (ChPT). In order to extract the strange quark mass we have used both the kaon mass and the mass of the (unphysical) η_s meson composed of two degenerate valence strange quarks. In both cases, the ultimate physical input is the kaon mass, together with the pion mass and decay constant.

For the charm quark mass, similarly to the strange quark, we have investigated several experimental inputs to extract its value: the mass of the D , D_s , and η_c mesons. In the charm quark sector discretization effects require some care and having data at four lattice spacings helps in performing the continuum limit.

The results that we obtain for the quark masses are, in the modified minimal subtraction ($\overline{\text{MS}}$) scheme,

$$\begin{aligned}\bar{m}_{ud}(2 \text{ GeV}) &= 3.6(1)(2) \text{ MeV} = 3.6(2) \text{ MeV}, \\ \bar{m}_s(2 \text{ GeV}) &= 95(2)(6) \text{ MeV} = 95(6) \text{ MeV}, \\ \bar{m}_c(\bar{m}_c) &= 1.28(3)(3) \text{ GeV} = 1.28(4) \text{ GeV},\end{aligned}\quad (1)$$

where the two separate errors are, respectively, statistical and systematic. We also obtain for the ratios of quark masses the values

$$m_s/m_{ud} = 27.3(5)(7) = 27.3(9), \quad m_c/m_s = 12.0(3), \quad (2)$$

which are independent of both the renormalization scheme and scale.

II. SIMULATION DETAILS

The calculation is based on the $N_f = 2$ gauge field configurations generated by the ETMC with the tree-level improved Symanzik gauge action [11] and the twisted-mass quark action [12] at maximal twist, discussed in detail in [9,13–16]. We simulated $N_f = 2$ dynamical quarks, taken to be degenerate in mass, whose masses are eventually extrapolated to the physical isospin averaged mass of the up and down quarks. As already mentioned, the strange and charm quarks are quenched in the present calculation.

The use of the twisted-mass fermions turns out to be beneficial, since the pseudoscalar meson masses, which represent the basic ingredient of the calculation, are automatically improved at $\mathcal{O}(a)$ [17]. As discussed in [10,18,19], we implement nondegenerate valence quarks in the twisted-mass formulation by formally introducing a twisted doublet for each nondegenerate quark flavor. In the present analysis we thus include in the valence sector three

twisted doublets, (u, d) , (s, s') , and (c, c') , with masses μ_l , μ_s , and μ_c , respectively. Within each doublet, the two valence quarks are regularized in the physical basis with Wilson parameters of opposite values, $r = -r' = 1$. Moreover, we only consider in the present study pseudo-scalar mesons composed of valence quarks regularized with opposite r . This choice guarantees that the squared meson mass m_{PS}^2 differs from its continuum counterpart only by terms of $\mathcal{O}(a^2 \mu_q)$ and $\mathcal{O}(a^4)$ [20,21].

Details of the ensembles of gauge configurations used in the present analysis and the values of the simulated valence quark masses are collected in Tables I and II, respectively. In order to investigate the properties of the various light, strange, and charmed mesons, we simulate the sea and valence up/down quark mass in the range $0.15m_s^{\text{phys}} \lesssim \mu_l \lesssim 0.5m_s^{\text{phys}}$, the valence strange quark mass within $0.8m_s^{\text{phys}} \lesssim \mu_s \lesssim 1.5m_s^{\text{phys}}$, and the valence charm quark mass within $0.9m_c^{\text{phys}} \lesssim \mu_c \lesssim 2.0m_c^{\text{phys}}$, with m_s^{phys} and m_c^{phys} being the physical strange and charm masses. Quark propagators with different valence masses are obtained using the so-called multiple mass solver method [22,23], which allows inverting the Dirac operator for several valence masses at a relatively low computational cost.

The statistical accuracy of the meson correlators is significantly improved by using the so-called ‘‘one-end’’ stochastic method, implemented in [24], which includes all spatial sources at a single time slice. Statistical errors on the meson masses are evaluated using the jackknife procedure. With 16 jackknife bins for each configuration ensemble we have verified that autocorrelations are well under control. Statistical errors on the fit results which are based on data obtained from independent ensembles of gauge configurations are evaluated using a bootstrap

TABLE I. Details of the ensembles of gauge configurations used in the present study: value of the gauge coupling β ; value of the lattice spacing a ; lattice size $V = L^3 \times T$ in lattice units; bare sea quark mass in lattice units; approximate value of the pion mass; approximate value of the product $m_\pi L$; number of independent configurations N_{cfg} .

Ensemble	β	$a[\text{fm}]$	V/a^4	$a\mu_{\text{sea}}$	$m_\pi[\text{MeV}]$	$m_\pi L$	N_{cfg}
A_2	3.8	0.098	$24^3 \times 48$	0.0080	410	5.0	240
A_3				0.0110	480	5.8	240
B_1	3.9	0.085	$24^3 \times 48$	0.0040	315	3.3	480
B_2				0.0064	400	4.1	240
B_3				0.0085	450	4.7	240
B_4				0.0100	490	5.0	240
B_7	3.9	0.085	$32^3 \times 64$	0.0030	275	3.7	240
B_6				0.0040	315	4.3	240
C_1	4.05	0.067	$32^3 \times 64$	0.0030	300	3.3	240
C_2				0.0060	420	4.5	240
C_3				0.0080	485	5.2	240
D_1	4.2	0.054	$48^3 \times 96$	0.0020	270	3.5	80
D_2		0.054	$32^3 \times 64$	0.0065	495	4.3	240

TABLE II. Values of simulated bare quark masses in lattice units for each configuration ensemble in the light, strange, and charm sectors.

	$a\mu_l$	$a\mu_s$	$a\mu_c$
A_2 – A_3	0.0080, 0.0110	0.0165, 0.0200 0.0250, 0.0300	0.2143, 0.2406 0.2701, 0.3032
B_1 – B_4	0.0040, 0.0064, 0.0085, 0.0100	0.0150, 0.0180 0.0220, 0.0270	0.2049, 0.2300 0.2582, 0.2898
B_7	0.0030	0.0150, 0.0180 0.0220, 0.0270	0.2049, 0.2300 0.2582, 0.2898
B_6	0.0040	0.0150, 0.0180 0.0220, 0.0270	0.2049, 0.2300 0.2582, 0.2898
C_1 – C_3	0.0030, 0.0060, 0.0080	0.0120, 0.0135 0.0150, 0.0180	0.1663, 0.1867 0.2096, 0.2352
D_1	0.0020	0.0130, 0.0150 0.0180	0.1670, 0.1920 0.2170
D_2	0.0065	0.0100, 0.0120 0.0150, 0.0190	0.1700, 0.2200 0.2700

procedure, with 100 bootstrap samples, which properly takes into account cross correlations.

The analysis is based on a study of the dependence of meson masses on renormalized quark masses, with data at the four simulated values of the lattice spacing simultaneously analyzed. For the quark mass renormalization constants $Z_\mu = Z_P^{-1}$ we use the results obtained in [7], which read

$$Z_P|_\beta = \{0.411(12), 0.437(7), 0.477(6)\}$$

$$\text{at } \beta = \{3.8, 3.9, 4.05\}, \quad (3)$$

in the $\overline{\text{MS}}$ scheme at 2 GeV. The errors given in Eq. (3) are those quoted in [7] and do not account either for discretization errors or for the uncertainty associated with the perturbative conversion from the regularization independent momentum–subtraction renormalization (RI-MOM) to the $\overline{\text{MS}}$ scheme. The former are taken care of by performing on the renormalized quark masses the extrapolation to the continuum limit. The uncertainty associated with the conversion from the RI-MOM to the $\overline{\text{MS}}$ scheme is included in our final estimate of the systematic error on the quark masses and will be discussed in Sec. III. For the renormalization constant at $\beta = 4.2$, not calculated in [7], we use the preliminary result $Z_P^{\overline{\text{MS}}}(2 \text{ GeV})|_{4.2} = 0.501(20)$, where the conservative uncertainty is due to the preliminary nature of the result.

The uncertainty on Z_P has been taken into account by including in the definition of the χ^2 to be minimized in the fits a term

$$\frac{(\tilde{Z}_P^i(a) - Z_P^i(a))^2}{\delta Z_P(a)^2}, \quad (4)$$

for each value of the lattice spacing and for each bootstrap sample, where $Z_P^i(a) \pm \delta Z_P(a)$ is the input value for the renormalization constant at the lattice spacing a and for the bootstrap i , and $\tilde{Z}_P^i(a)$ the corresponding fit parameter. This procedure corresponds to assuming for the renormalization constant a Bayesian Gaussian prior [9,25].

The simultaneous analysis of data at different values of the lattice spacing also requires the data conversion from lattice units to a common scale. For the analysis in the pion sector, we have expressed all dimensionful quantities in units of the Sommer parameter r_0 [26]. We use for r_0/a in the chiral limit the values

$$\left. \frac{r_0}{a} \right|_\beta = \{4.54(7), 5.35(4), 6.71(4), 8.36(6)\}$$

$$\text{at } \beta = \{3.8, 3.9, 4.05, 4.2\}, \quad (5)$$

obtained from an extension of the analyses in [9,14] with the inclusion of all four lattice spacings. As in [9], the chiral extrapolation of r_0/a is performed by using three *Ansätze* for the sea quark mass dependence: linear only, quadratic only, and quadratic + linear. The size of mass-dependent discretization effects is verified by including in the fits $\mathcal{O}(a^2 m_l)$ and $\mathcal{O}(a^2 m_l^2)$ terms, which turn out to be negligible. The uncertainties on the results given in Eq. (5) include the systematic errors estimated as the spread among the values obtained from the above-mentioned fits. In the present analysis the uncertainty on the r_0/a values is taken into account by adding a term to the χ^2 of the fit in a similar way to Z_P , as explained above.

The analysis in the pion sector is also used to determine, besides the value of the average up/down quark mass at the physical point, the lattice spacing at each coupling β . The physical input used for this determination is the pion decay constant f_π . In the successive determination of the strange

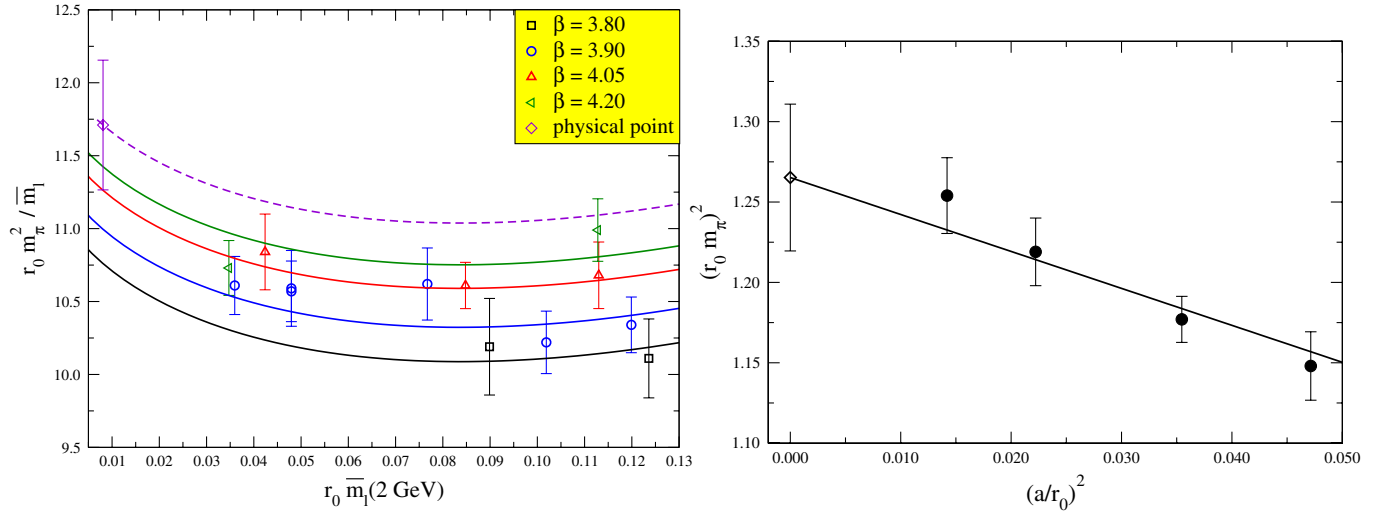


FIG. 1 (color online). Left: Dependence of $r_0 m_\pi^2 / \bar{m}_l$ on the renormalized light quark mass at the four lattice spacings. Right: Dependence of $(r_0 m_\pi)^2$ on the squared lattice spacing, for a fixed reference light quark mass ($\bar{m}_{ud}^{\text{ref}} = 50$ MeV). Empty diamonds represent continuum limit results.

and charm quark masses, the data are analyzed directly in physical units.

III. UP/DOWN QUARK MASS

The calculation of the up/down quark mass follows the strategy of [9]. The analysis is repeated here including simultaneously all data available at the four values of the lattice spacing.

We have studied the dependence of the pion mass and decay constant on the renormalized quark mass. For these quantities the predictions based on next-to-leading order (NLO) ChPT and the Symanzik expansion up to $\mathcal{O}(a^2)$ can be written in the form

$$\begin{aligned}
 m_\pi^2 &= (2B_0 m_l) \cdot \left[1 + \frac{2B_0 m_l}{16\pi^2 f_0^2} \log\left(\frac{2B_0 m_l}{16\pi^2 f_0^2}\right) \right. \\
 &\quad \left. + P_1 m_l + a^2 \cdot \left(P_2 + P_3 \log\left(\frac{2B_0 m_l}{16\pi^2 f_0^2}\right) \right) \right], \\
 f_\pi &= f_0 \cdot \left[1 - 2 \frac{2B_0 m_l}{16\pi^2 f_0^2} \log\left(\frac{2B_0 m_l}{16\pi^2 f_0^2}\right) \right. \\
 &\quad \left. + P_4 m_l + a^2 \cdot \left(P_5 + P_6 \log\left(\frac{2B_0 m_l}{16\pi^2 f_0^2}\right) \right) \right], \quad (6)
 \end{aligned}$$

where m_l is the renormalized light quark mass and B_0 and f_0 are the low energy constants entering the leading order (LO) chiral Lagrangian.¹

The coefficients of the discretization terms of $\mathcal{O}(a^2 m_l \log(m_l))$ receive a contribution from the $\mathcal{O}(a^2)$

¹The pseudoscalar decay constant in the chiral limit, f_0 , is normalized such that $f_\pi = 130.7$ MeV at the physical point.

splitting between the neutral and charged pion (squared) mass, $\Delta m_\pi^2 = m_{\pi^0}^2 - m_{\pi^\pm}^2$, which occurs with twisted-mass fermions. This contribution has been recently evaluated in [27]. Our main results are obtained through a fit of Eq. (6), with the coefficients P_3 and P_6 obtained by expanding the results of [27] up to $\mathcal{O}(a^2)$. We have also verified that the results obtained in this way are indistinguishable from those obtained using directly the resummed formulas of [27]. From our fit, the splitting Δm_π^2 turns out to be determined with an uncertainty of approximately 60%. We obtain $\Delta m_\pi^2 = -(33 \pm 19)a^2 \Lambda_{\text{QCD}}^4$, which is consistent with a direct ETMC determination performed with two lattice spacings ($\Delta m_\pi^2 = -50a^2 \Lambda_{\text{QCD}}^4$ [28]). On the final result for the light quark mass the impact of this correction is at the level of the fitting error.

Lattice results for pion masses and decay constants have been corrected for finite size effects (FSEs) evaluated using the resummed Lüscher formulas. The effect of the $\mathcal{O}(a^2)$ isospin breaking has been taken into account also in these corrections [29]. On our pion data, FSEs vary between 0.2% and 2%, depending on the simulated mass and volume. The inclusion of the pion mass splitting in the FSEs induces a variation of about 15%–40% in the finite size correction itself. This effect is at the level of one-third of the statistical error for our lightest pion mass at $\beta = 3.9$ on the smaller volume, and even smaller in the other cases.

In Fig. 1 (left) we show the dependence of $r_0 m_\pi^2 / m_l$ on the renormalized light quark mass at the four β 's, and the curves corresponding to the best fit of the lattice data according to Eq. (6).

In order to illustrate the dependence of the pion mass on the lattice cutoff, we have interpolated the lattice data for m_π^2 at the four values of the lattice spacing to a common reference value of the light quark mass, $\bar{m}_{ud}^{\text{ref}} = 50$ MeV. The resulting values of $(r_0 m_\pi)^2$ obtained in this way are

shown in Fig. 1 (right) as a function of a^2 , together with the corresponding continuum extrapolation. We see that discretization errors on the pion mass square are below 10% at $\beta = 3.9$ and negligible within the fitting errors at $\beta = 4.2$.

The value of the physical up/down quark mass is extracted from the ratio m_π^2/f_π^2 using as an input the experimental value of the latter ratio.² In order to estimate the systematic uncertainty due to discretization effects we have performed both a fit without the logarithmic discretization terms, i.e., with $P_3 = P_6 = 0$ in Eq. (6) (the so-called fit B of [9]), and a fit without all $\mathcal{O}(a^2)$ corrections, i.e., with $P_2 = P_3 = P_5 = P_6 = 0$ (the so-called fit A of [9]). Both these *Ansätze* turn out to be compatible with the lattice data. We find that the result for the up/down quark mass decreases by approximately 2% and increases by about 6% in the two cases, respectively, so that we estimate an overall uncertainty due to residual discretization effects of $\pm 4\%$. We have also tried to add in the fit discretization terms of $\mathcal{O}(a^2 m_l^2)$ or $\mathcal{O}(a^4)$. In both cases these terms turn out to be hardly determined with our data, leading for m_{ud} to results consistent with those obtained from the other fits, but with uncertainties larger by a factor 3.

For estimating the systematic uncertainty due to the chiral extrapolation we have also considered a fit including a next-to-next-to-leading order local contribution proportional to the light quark mass square. In this case we are not able to determine all the fitting parameters and we are thus forced to introduce, on the additional low energy constants, priors as in [9]. In this way we find that the result for m_{ud} increases by 6%.

The results of the fits described above are collected in Table III in the Appendix.

As anticipated in the previous section, we also include in the final result a systematic uncertainty coming from the perturbative conversion of the quark mass renormalization constant from the RI-MOM to the $\overline{\text{MS}}$ scheme. Using the results of the 3-loop calculation of [31], one can write the relation between the quark mass in the two schemes as

$$\frac{\bar{m}(\mu)}{m^{\text{RI}}(\mu)} = 1 - 0.424\alpha_s(\mu) - 0.827\alpha_s(\mu)^2 - 2.126\alpha_s(\mu)^3 + \mathcal{O}(\alpha_s(\mu)^4). \quad (7)$$

The uncertainty due to the truncation of the perturbative series has been conservatively estimated by assuming the

²In order to account for the electromagnetic isospin breaking effects which are not introduced in the lattice simulation, we have used in the present analysis as “experimental” values of the pion and kaon mass the combinations [30]

$$(M_\pi^2)_{\text{QCD}} = M_{\pi^0}^2, \\ (M_K^2)_{\text{QCD}} = \frac{1}{2}[M_{K^0}^2 + M_{K^+}^2 - (1 + \Delta_E)(M_{\pi^+}^2 - M_{\pi^0}^2)],$$

with $\Delta_E = 1$. The values of the experimental inputs for the pion and kaon masses are then $m_\pi^{\text{exp}} = 135.0$ MeV, $m_K^{\text{exp}} = 494.4$ MeV.

unknown $\mathcal{O}(\alpha_s^4)$ term to be as large as the $\mathcal{O}(\alpha_s^3)$ one. Evaluating this term at the renormalization scale $\mu \simeq 3$ GeV, which is the typical scale of the nonperturbative RI-MOM calculation in our simulation [7], and using $\alpha_s(3 \text{ GeV}, N_f = 2) = 0.202$, we then find that this uncertainty corresponds to approximately $\pm 2\%$.

Adding in quadrature the three systematic errors discussed above we obtain $\bar{m}_{ud} = 3.55(14)_{(-16)}^{(+28)}$ MeV in the $\overline{\text{MS}}$ scheme at the renormalization scale of 2 GeV, where the two errors are statistical and systematic, respectively. Finally we symmetrize the error, obtaining

$$\bar{m}_{ud}(2 \text{ GeV}) = 3.6(1)(2) \text{ MeV} = 3.6(2) \text{ MeV}. \quad (8)$$

Note that, in the symmetrized result, the uncertainties due to discretization effects, chiral extrapolation, and perturbative conversion give similar contributions to the final systematic error, at the level of 4%, 3%, and 2%, respectively.

Using as an input the experimental value of the pion decay constant, the fits also provide us with the values of lattice spacing at the four simulated β 's, which are used in the rest of the analysis. They read, at $\beta = \{3.8, 3.9, 4.05, 4.2\}$, respectively,

$$a|_\beta = \{0.098(3)(2), 0.085(2)(1), \\ 0.067(2)(1), 0.054(1)(1)\} \text{ fm}, \quad (9)$$

where again the two errors are statistical and systematic. The results in Eqs. (8) and (9) are in good agreement with the previous ETMC determination obtained in [9] from the analysis of data at $\beta = 3.8, 3.9$, and 4.05.

We observe that, in principle, the ratio of lattice spacings at two different β values could be determined from the fit of the pion meson mass and decay constant, without using the additional information coming from the values of r_0/a of Eq. (5). With our data, however, the uncertainties on the values of the quark mass renormalization constant, as well as the *a priori* unknown size of discretization errors affecting the pion masses and decay constants, do not allow us to achieve a reliable determination of these ratios.

IV. STRANGE QUARK MASS

In this section, we first present the determination of the strange quark mass based on the study of the kaon meson mass. The alternative determination based on the study of the η_s meson will be discussed later on.

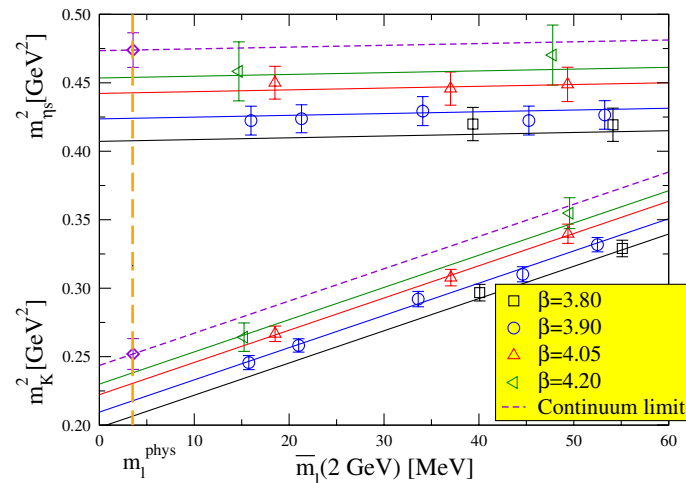
Since the valence strange quark mass has not been previously tuned in our simulation, the determination of the physical strange quark mass requires an interpolation of the lattice data. As already mentioned, for all values of the lattice couplings, the simulated values of the strange quark masses are approximately in the range $0.8m_s^{\text{phys}} \leq \mu_s \leq 1.5m_s^{\text{phys}}$.

In order to better discriminate the strange quark mass dependence of the kaon masses on other dependencies, in particular, discretization effects, we firstly slightly

interpolate the lattice data to three reference values of the strange quark mass, which are chosen to be equal at the four lattice spacings: $\bar{m}_s^{\text{ref}} = \{80, 95, 110\}$ MeV. The interpolations to the reference masses are performed by using quadratic spline fits. Then, at fixed reference strange mass, we simultaneously study the kaon mass dependence on the up/down quark mass and on discretization effects, thus performing the chiral extrapolation and taking the continuum limit. In this step, we have considered chiral fits based either on SU(2)-ChPT [3,32], where the chiral symmetry is assumed for the up/down quark only, or on partially quenched SU(3)-ChPT [33], where instead also the valence strange quark is treated as light. In order to extrapolate the kaon mass values to the continuum and to the physical m_{ud} limit, we use the results for the average up/down quark mass and for the lattice spacings obtained in Eqs. (8) and (9), at each reference value of the strange quark mass. Finally, we study the kaon mass dependence on the strange quark mass, and determine the value of the physical strange quark mass using the experimental value of m_K .

Let us describe the chiral fits in more detail. As discussed above, fits are performed in two steps: (1) the strange quark mass is fixed to the reference values and only the m_l and a^2 dependence of the kaon mass is studied; (2) the so obtained data in the continuum limit and at the physical m_{ud} value are studied as a function of the strange quark mass. In these two steps, we have considered for the kaon meson mass functional forms based on the predictions of either NLO SU(2)-ChPT [3], which predicts the absence at this order of chiral logs,

$$(1) \quad m_K^2(m_s, m_l, a) = Q_1(m_s) + Q_2(m_s)m_l + Q_3(m_s)a^2, \quad \forall m_s, \quad (10)$$



$$(2) \quad m_K^2(m_s, m_l^{\text{phys}}, a = 0) \equiv Q_1(m_s) + Q_2(m_s)m_l^{\text{phys}} = Q_4 + Q_5 m_s, \quad (11)$$

or SU(3)-ChPT [33]

$$(1) \quad m_K^2(m_s, m_l, a) = B_0 \cdot (m_s + m_l) \cdot (1 + Q_6(m_s) + Q_7(m_s)m_l + Q_8(m_s)a^2), \quad \forall m_s, \quad (12)$$

$$(2) \quad m_K^2(m_s, m_l^{\text{phys}}, a = 0) \equiv B_0 \cdot (m_s + m_l^{\text{phys}}) \cdot (1 + Q_6(m_s) + Q_7(m_s)m_l^{\text{phys}}) = B_0 \cdot (m_s + m_l^{\text{phys}}) \cdot \left(1 + \frac{2B_0 m_s}{(4\pi f_0)^2} \log \frac{2B_0 m_s}{(4\pi f_0)^2} + Q_9 m_s\right), \quad (13)$$

where B_0 and f_0 are determined from the pion fit described in the previous section. Note that the dependence of the kaon mass on the strange quark mass is not determined by the chiral symmetry in the SU(2) theory. We find that, with our choice of three reference strange masses around the physical value, a linear fit as given in Eq. (11) is perfectly adequate to describe the data.

For illustration we show in Fig. 2 the combined chiral/continuum fit based on SU(2)-ChPT, Eq. (10), for a fixed reference value of the strange quark mass, as a function of the light quark mass (left) and of the squared lattice spacing (right). In Fig. 3 the dependence on the strange quark mass is shown, in the case of the SU(2) analysis [see Eq. (11)]. The dependencies are shown for the kaon squared mass as well as for the η_s squared mass discussed hereafter.

As an alternative way to determine the strange quark mass we have studied the dependence on m_s of a meson made up of two strange valence quarks [5]. The advantage

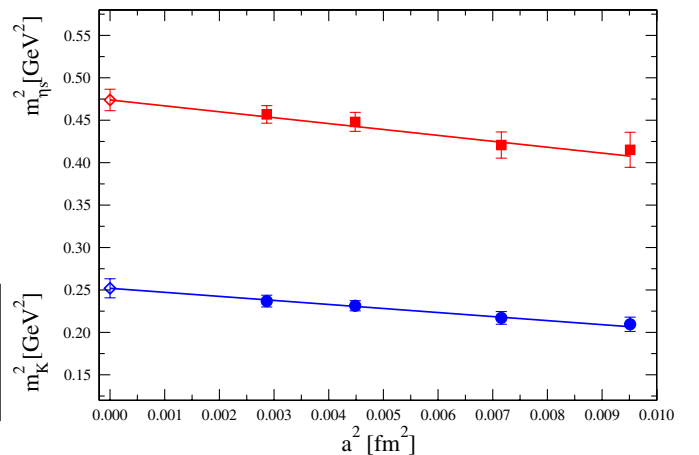


FIG. 2 (color online). Left: Dependence of m_K^2 and $m_{\eta_s}^2$ on the renormalized light quark mass, for a fixed reference strange quark mass ($\bar{m}_s^{\text{ref}} = 95$ MeV) and at the four lattice spacings. The orange vertical line corresponds to the physical up/down mass. Right: Dependence of m_K^2 and $m_{\eta_s}^2$ on the squared lattice spacing, for a fixed reference strange quark mass ($\bar{m}_s^{\text{ref}} = 95$ MeV) and at the physical up/down mass. Empty diamonds represent continuum limit results.

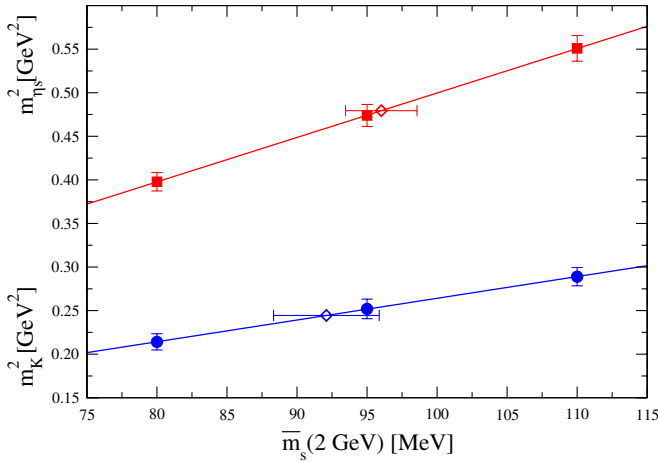


FIG. 3 (color online). Dependence of m_K^2 and $m_{\eta_s}^2$, in the continuum limit and at the physical up/down mass, on the strange quark mass. The strange mass results obtained from the SU(2)-ChPT analyses of kaon and η_s mesons are also shown, with empty diamonds.

of this approach is that the mass of this unphysical meson, denoted as η_s , is only sensitive to the up/down quark mass through sea quark effects, and it is thus expected to require only a very smooth chiral extrapolation. This expectation will be confirmed by our analysis. The price to pay is the need for an additional chiral fit required to determine the η_s mass at the physical point.

In the real world, the η_s meson is known to mix with the $(\bar{u}u + \bar{d}d)$ component to produce the physical η and η' mesons. This mixing proceeds through the contribution of disconnected diagrams, which are known to be rather noisy on the lattice and therefore computationally expensive. In order to avoid this computation we consider here the two strange quarks composing the meson as degenerate in mass but distinct in flavor. Though this η_s meson does not exist in nature, its mass can be determined on the lattice [5].

In order to relate the mass of the η_s meson to the physically observable m_π and m_K , we have studied its dependence on the kaon and pion masses for different values of the simulated light and strange quark masses. This dependence turns out to be well described by both the functional form³ based on either NLO SU(2)-ChPT,

$$m_{\eta_s}^2 = R_1 + R_2(2m_K^2 - m_\pi^2) + R_3m_\pi^2 + R_4a^2, \quad (14)$$

or SU(3)-ChPT,

³The functional forms in Eqs. (14) and (15) are obtained from the ChPT formulas given in Eqs. (17)–(20) by replacing quark masses in terms of meson masses, and keeping terms up to NLO.

$$m_{\eta_s}^2 = (2m_K^2 - m_\pi^2) \cdot [1 + (\xi_s - \xi_l) \log(2\xi_s) + (R_7 + 1)(\xi_s - \xi_l) + R_8a^2] - m_\pi^2[-\xi_l \log(2\xi_l) + \xi_s \log(2\xi_s) + R_7(\xi_s - \xi_l)], \quad (15)$$

with $\xi_l = m_\pi^2/(4\pi f_0)^2$ and $\xi_s = (2m_K^2 - m_\pi^2)/(4\pi f_0)^2$. We observe that, within the accuracy of our lattice data, the $\mathcal{O}(a^2)$ term in the η_s mass is found to be independent of the strange quark mass.

Once the physical values of the kaon and pion mass are inserted in Eqs. (14) and (15), we find that the two fits yield very close results for the η_s meson mass, namely,

$$\begin{aligned} m_{\eta_s} &= 692(1) \text{ MeV} && \text{from SU(2),} \\ m_{\eta_s} &= 689(2) \text{ MeV} && \text{from SU(3),} \end{aligned} \quad (16)$$

to be compared with the LO SU(3) prediction $(m_{\eta_s})_{\text{LO}} = \sqrt{2m_K^2 - m_\pi^2} = 686 \text{ MeV}$ and with the lattice determination of [5] $m_{\eta_s} = 686(4) \text{ MeV}$.

Once the mass of the η_s meson has been determined, the strange quark mass can be extracted by following the very same procedure described for the case of the kaon mass. At first, lattice data at fixed reference strange mass are extrapolated to the continuum and to the physical up/down mass (see Fig. 2). After this extrapolation, the value of the physical strange quark mass is extracted by studying the dependence on the strange mass (see Fig. 3). We have considered the following fitting functions based on NLO ChPT for the dependence of the η_s meson (1) on the (sea) up/down quark mass and on the leading discretization effects, and (2) on the strange quark mass:

$$(1) \quad m_{\eta_s}^2(m_s, m_l, a) = T_1(m_s) + T_2(m_s)m_l + T_3(m_s)a^2, \quad \forall m_s, \quad (17)$$

$$(2) \quad m_{\eta_s}^2(m_s, m_l^{\text{phys}}, a = 0) \equiv T_1(m_s) + T_2(m_s)m_l^{\text{phys}} = T_4 + T_5m_s, \quad (18)$$

in SU(2), and

$$(1) \quad m_{\eta_s}^2(m_s, m_l, a) = 2B_0m_s \cdot (1 + T_6(m_s) + T_7(m_s)m_l + T_8(m_s)a^2), \quad \forall m_s, \quad (19)$$

$$(2) \quad m_{\eta_s}^2(m_s, m_l^{\text{phys}}, a = 0) \equiv 2B_0m_s \cdot (1 + T_6(m_s) + T_7(m_s)m_l^{\text{phys}}) = 2B_0m_s \cdot \left(2 \frac{2B_0m_s}{(4\pi f_0)^2} \log\left(2 \frac{2B_0m_s}{(4\pi f_0)^2} \right) + T_9 + T_{10}m_s \right), \quad (20)$$

in SU(3). The low energy constants T_2 and T_7 , describing the dependence on the light quark mass, are found to be

independent of the strange mass, within the accuracy of our lattice data. They are then fitted with a single parameter for all reference strange quark masses.

The results for the strange quark mass obtained from both the kaon and the η_s meson masses turn out to be consistent, as can be seen from Table IV in the Appendix where the several m_s values obtained from different fits are collected.

In order to quote a final estimate for the strange quark mass we choose as a central value the weighted average of the results from the four determinations discussed above, namely, from K and η_s and based on SU(2)- and SU(3)-ChPT. In the $\overline{\text{MS}}$ scheme at 2 GeV this average reads $\bar{m}_s(2 \text{ GeV}) = 95(2) \text{ MeV}$, with the 2 MeV error representing the typical statistical and fitting uncertainty. The difference between the determinations based on the K and η_s mesons is about 3%. The results obtained from either the SU(2) or the SU(3) fits are practically the same in the analysis based on the η_s and differ by approximately 3% in the kaon case. In order to evaluate the uncertainty of the continuum extrapolation we have proceeded in two ways. We have either added an $\mathcal{O}(a^4)$ mass independent term in Eqs. (10), (12), (17), and (19) or excluded from these fits the data from the coarser lattice (with $a \approx 0.098 \text{ fm}$). We find that the $\mathcal{O}(a^4)$ term turns out to be hardly determined in the fit, leading to a factor 3 larger uncertainties. The exclusion of $\beta = 3.8$ data, instead, yields a variation of the results of approximately 2% leaving the fitting error approximately unchanged. We then assume $\pm 2\%$ as uncertainty related to the continuum extrapolation. The different fits considered for the determination of the up/down mass and of the lattice spacing affect the determination of the strange mass at the level of 3%. Finally, we include also in this case an uncertainty of 2% related to the truncation of the perturbative expansion in the conversion from the RI-MOM to the $\overline{\text{MS}}$ scheme. Combining all these uncertainties in quadrature, we quote as our final estimate of the strange quark mass in the $\overline{\text{MS}}$ scheme

$$\bar{m}_s(2 \text{ GeV}) = 95(2)(6) \text{ MeV} = 95(6) \text{ MeV}. \quad (21)$$

We observe that our result for the strange mass in Eq. (21) is, though compatible, smaller than the value obtained in [10] at a fixed value of the lattice spacing ($a \approx 0.085 \text{ fm}$). This is a consequence of discretization effects, which are at the level of 15% in m_K^2 on the $a \approx 0.085 \text{ fm}$ lattice, as shown in Fig. 2 (right). A further comparison can be done with the ETMC estimate of the strange quark mass that appeared in the recent work on the bag parameter B_K [34]. Within that analysis, based on data at three β values (3.8, 3.9, and 4.05), the strange quark mass is determined from the same lattice setup by performing an SU(2) chiral fit of the kaon meson mass. The result obtained in [34] reads $\bar{m}_s(2 \text{ GeV}) = 92(5) \text{ MeV}$, to be compared to our result $\bar{m}_s(2 \text{ GeV}) = 92.1(3.8) \text{ MeV}$, obtained from the same fit (see Table IV).

Using our determinations of both the strange and light quark masses, we can obtain a prediction for the ratio m_s/m_{ud} , which is both a scheme and scale independent quantity. The several m_s/m_{ud} values obtained from different fits are collected in Table V in the Appendix.⁴ The result that we quote as our final estimate is

$$m_s/m_{ud} = 27.3(5)(7) = 27.3(9). \quad (22)$$

V. CHARM QUARK MASS

The determination of the charm quark mass follows, quite closely, the strategy adopted in the determination of the strange quark mass discussed in the previous section. In this case, we use as experimental input the masses of the D , D_s , and η_c mesons.

As for the strange quark case, the analysis requires an interpolation of the lattice data, being the simulated charm masses roughly in the range $0.9m_c^{\text{phys}} \lesssim \mu_c \lesssim 2.0m_c^{\text{phys}}$. In order to better study the a^2 and m_l dependence of charmed meson masses, we first use a quadratic spline fit to interpolate the data at three reference values of the charm mass which are equal at the four β values: $\bar{m}_c^{\text{ref}}(2 \text{ GeV}) = \{1.08, 1.16, 1.24\} \text{ GeV}$. We have verified that a different choice of the values of the reference masses leaves the charm quark results unchanged. At fixed reference charm mass, we then study the dependence of the D , D_s , and η_c meson on the up/down mass (and on the strange mass in the case of the D_s meson) and on discretization terms, thus getting the results for the meson masses in the continuum limit, at the physical values of the light (and strange) quark masses, and at the reference charm mass. Finally, the value of the physical charm quark mass is extracted by fitting these data as a function of the charm quark mass and using as an input the experimental value of the corresponding charmed meson $m_D^{\text{exp}} = 1.870 \text{ GeV}$, $m_{D_s}^{\text{exp}} = 1.969 \text{ GeV}$, $m_{\eta_c}^{\text{exp}} = 2.981 \text{ GeV}$.⁵

In order to fit the meson masses we have considered the following (phenomenological) polynomial fits, which turn out to describe well the dependence on the light and strange quark masses and on the lattice cutoff of the D , D_s , and η_c meson masses, at fixed (reference) charm mass m_c ,

⁴The results for the ratio m_s/m_{ud} collected in Table V are slightly different from the ratios of the \bar{m}_s and \bar{m}_{ud} results. This difference originates from the fact that in the ratio m_s/m_{ud} the quark mass renormalization constant Z_P^{-1} exactly cancels out, whereas in the determinations of \bar{m}_s and \bar{m}_{ud} the central values of Z_P are slightly modified by the fitting procedure.

⁵The experimental value of the meson masses should be corrected to take into account the absence of electromagnetic effects and, in the case of the η_c , of disconnected diagrams in the lattice calculation. For the η_c meson, these corrections are estimated to be of the order of 5 MeV [5], thus affecting the extracted charm quark mass to approximately 0.2%. Similar corrections are expected for the D and D_s mesons. Given our uncertainties, we can safely neglect these corrections in the analysis.

$$\begin{aligned}
 m_H(m_c, m_s, m_l, a) &= C_1^H(m_c) + C_2^H(m_c)m_l \\
 &+ C_3^H(m_c)m_s + C_4^H(m_c)a^2, \quad \forall m_c,
 \end{aligned}
 \quad (23)$$

with $H = D, D_s, \eta_c$. From the fits, we find that the coefficients C_2^H and C_3^H turn out to be independent of the charm mass within the statistical errors. The latter coefficient C_3^H , of course, enters the fit only in the D_s case.

For the charm mass dependence, a constant plus either a linear or a $1/m_c$ term have been considered for describing data of the D, D_s , and η_c mesons, namely,

$$\begin{aligned}
 m_H(m_c, m_s^{\text{phys}}, m_l^{\text{phys}}, a = 0) \\
 &\equiv C_1^H(m_c) + C_2^H(m_c)m_l^{\text{phys}} + C_3^H(m_c)m_s^{\text{phys}} \\
 &= C_5^H + \frac{C_6^H}{m_c} + C_7^H m_c.
 \end{aligned}
 \quad (24)$$

Since we have data at three reference charm masses (close to the physical charm), we can keep only one of the coefficients C_6^H, C_7^H different from zero. We find that both choices describe very well the lattice data and affect only in a marginal way the interpolation to the physical charm mass.

In Fig. 4 we show the dependence of the D, D_s , and η_c masses on the light quark mass at a fixed reference charm mass, for the four β 's. For the D_s and η_c mesons, which contain the light quark in the sea only, this dependence turns out to be practically invisible.

In Fig. 5 (left) the meson masses at physical light and strange quark masses are shown as a function of a^2 , for a reference value of the charm quark mass. As can be seen from this plot, discretization effects on the η_c meson mass vary from approximately 4% on the finest lattice up to 14% on the coarsest one. These effects are larger than those affecting the D and D_s meson masses by approximately 30%. Figure 5 (left) also shows that the dependence of the

three charmed meson masses on a^2 is very well described by a linear behavior, and attempts to vary the continuum extrapolation with respect to the simple linear fit produce only small effects. The latter are included in the estimate of the systematic uncertainty, as discussed below.

Finally, Fig. 5 (right) shows the dependence of the D, D_s , and η_c masses on the charm mass (in the continuum limit and at physical light and strange mass) and the interpolation to the physical charm.

Using the experimental values of the considered meson masses we get for the charm quark mass the results collected in Table VI.

In order to estimate the uncertainty due to the continuum extrapolation we have proceeded in two ways. We have either added in the fitting form of Eq. (23) an $\mathcal{O}(a^4)$ dependence, which turns out to be hardly determined thus leading to uncertainties larger by a factor 3, or excluded the data from the coarser lattice (with $a \simeq 0.098$ fm). This latter analysis yields a variation of the results of approximately 1.5%. The two dependencies of the meson masses on the charm quark mass, considered in Eq. (24), yield results that differ by only a few MeV. The systematic uncertainty then comes from the sum in quadrature of the approximately 1% spread among the three determinations from the D, D_s , and η_c mesons, the 1.5% uncertainty due to discretization effects, and the 2% uncertainty coming from the perturbative conversion of the renormalization constants from the RI-MOM to the $\overline{\text{MS}}$ scheme.

We quote as our final result for the charm quark mass in the $\overline{\text{MS}}$ scheme

$$\begin{aligned}
 \bar{m}_c(2 \text{ GeV}) &= 1.14(3)(3) \text{ GeV} = 1.14(4) \text{ GeV} \\
 &\rightarrow \bar{m}_c(\bar{m}_c) = 1.28(4) \text{ GeV},
 \end{aligned}
 \quad (25)$$

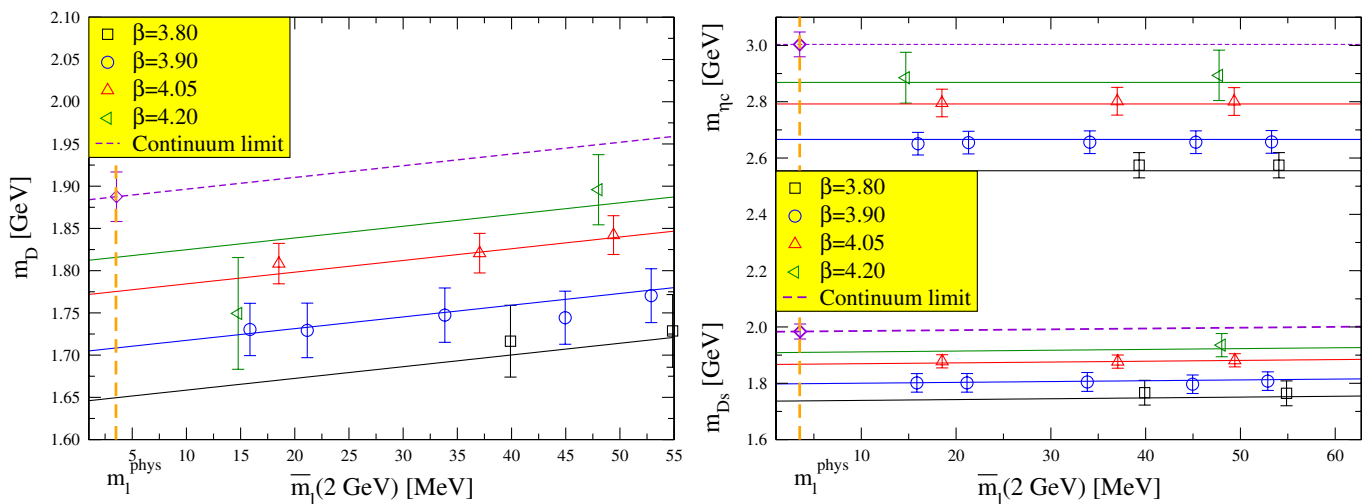


FIG. 4 (color online). Left: Dependence of m_D (left) and m_{D_s} and m_{η_c} (right) on the light quark mass, at fixed reference charm quark mass ($\bar{m}_c^{\text{ref}} = 1.16$ GeV) and for the four simulated lattice spacings. For the D_s meson the strange quark mass is fixed to the reference value $\bar{m}_s^{\text{ref}} = 95$ MeV.

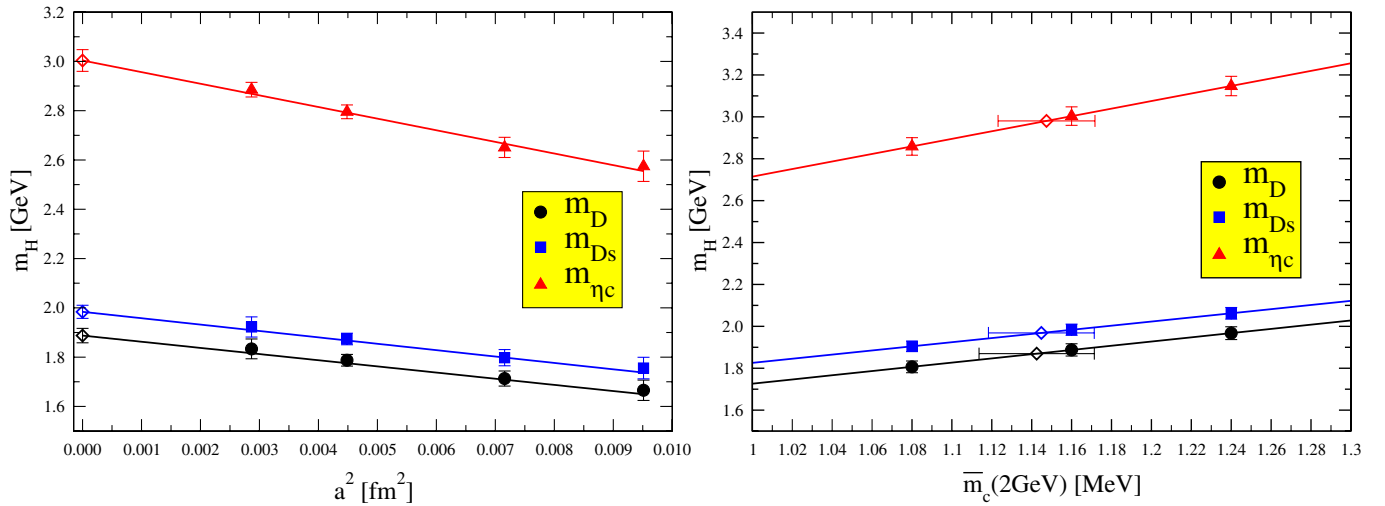


FIG. 5 (color online). Left: Dependence of m_D , m_{D_s} , and m_{η_c} , at fixed reference charm quark mass ($\bar{m}_c^{\text{ref}} = 1.16$ GeV) and at physical up/down and strange quark mass, on the squared lattice spacing. Empty diamonds represent continuum limit results. Right: Dependence of m_D , m_{D_s} , and m_{η_c} , in the continuum limit and at physical up/down and strange quarks, on the charm quark mass. The charm mass results from the three determinations are also shown, with empty diamonds.

where the evolution to the more conventional scale given by \bar{m}_c itself has been performed at N³LO [31] with $N_f = 2$, consistently with our nonperturbative evaluation of the renormalization constant. Had we evolved with $N_f = 4$, which is the number of active flavors above $\mu = m_c$, the result for $\bar{m}_c(\bar{m}_c)$ would have increased by less than 1 standard deviation.

Our result is compatible with the preliminary estimate of the charm quark mass, $\bar{m}_c(2\text{ GeV}) = 1.23(6)$, obtained by ETMC [35] using data at three lattice spacings and preliminary values for the renormalization constants. It is also in good agreement with the HPQCD result $\bar{m}_c(\bar{m}_c) = 1.268(9)$ GeV [6], with a larger uncertainty in our determination. Finally, our result is in good agreement with the recent sum rules determination $\bar{m}_c(\bar{m}_c) = 1.279(13)$ GeV of [36].

We also provide a prediction for the scheme and scale independent ratio m_c/m_s . The several m_c/m_s values obtained from different fits are collected in Table VII in the Appendix. The result that we quote as our final estimate is

$$m_c/m_s = 12.0(3), \quad (26)$$

in good agreement with the other recent lattice determination $m_c/m_s = 11.85(16)$ [5].

VI. CONCLUSIONS

We have presented results for the average up/down, strange, and charm quark masses, obtained with $N_f = 2$ twisted-mass Wilson fermions. The analysis includes data at four values of the lattice spacing and pion masses as low as ≈ 270 MeV, allowing a well controlled continuum limit and chiral extrapolation. Within the strange sector the

chiral extrapolation is performed by using either SU(2)- or SU(3)-ChPT. The strange and charm masses are extracted by using several methods, based on different meson mass inputs: the kaon and the η_s meson for the strange quark and the D , D_s , and η_c mesons for the charm. The quark mass renormalization is carried out nonperturbatively using the RI-MOM method.

The results for the quark masses in the $\overline{\text{MS}}$ scheme read: $\bar{m}_{ud}(2\text{ GeV}) = 3.6(2)$ MeV, $\bar{m}_s(2\text{ GeV}) = 95(6)$ MeV, and $\bar{m}_c(\bar{m}_c) = 1.28(4)$ GeV. The quoted errors include the uncertainty in the perturbative conversion of the renormalization constants from the RI-MOM to the $\overline{\text{MS}}$ scheme, which is conservatively estimated to be at the level of 2%. We emphasize that this uncertainty is not related to the lattice calculation itself, but comes from continuum perturbation theory. If the RI-MOM scheme was chosen as a reference scheme and, say, 3 GeV as a reference scale, which is the typical scale of the nonperturbative RI-MOM calculation in our lattice simulation [7], this uncertainty would not be present at all. For reference we provide our results for the quark masses also in this scheme: $m_{ud}^{\text{RI}}(3\text{ GeV}) = 3.9(1)(2)$ MeV, $m_s^{\text{RI}}(3\text{ GeV}) = 102(2)(6)$ MeV, and $m_c^{\text{RI}}(3\text{ GeV}) = 1.22(3)(2)$ GeV.

We have also evaluated the quark mass ratios $m_s/m_{ud} = 27.3(9)$ and $m_c/m_s = 12.0(3)$, which are independent on both the renormalization scale and scheme.

The only systematic uncertainty which is not accounted for by our results is the one stemming from the missing strange and charm quark vacuum polarization effects. A comparison, for instance, of our $N_f = 2$ result for the strange quark mass to already existing results from $N_f = 2 + 1$ quark flavor simulations [8] indicates that the error due to the partial quenching of the strange quark is smaller

at present than other systematic uncertainties. In this respect we mention that simulations with $N_f = 2 + 1 + 1$ dynamical flavors are already being performed by ETMC and preliminary results for several flavor physics observables have been recently presented [37,38].

ACKNOWLEDGMENTS

We thank all the ETMC members for fruitful discussions and the apeNEXT computer centers in Rome for their invaluable technical help. Some computation time has been used for that project on the BlueGene system at IDRIS. We are also grateful to Gilberto Colangelo for having provided us with a routine for the calculation of the FSEs [29], and to Chris Sachrajda for drawing our attention to the uncertainty in the perturbative conversion of the renormalization constants.

APPENDIX

We collect in this Appendix the results obtained for the up/down, strange, and charm quark masses from the different fits considered in the present analysis.

As discussed in Sec. III, in the light quark sector we have performed the following fits:

L1: this is our best fit which is based on NLO ChPT with the inclusion of $\mathcal{O}(a^2)$ discretization effects. This fit corresponds to Eq. (6) with all parameters different from zero.

L2: same as L1 but without discretization terms, i.e., $P_2 = P_3 = P_5 = P_6 = 0$ in Eq. (6).

L3: same as L1 with the inclusion of a next-to-next-to-leading order correction proportional to the square of the light quark mass.

The results for the up/down quark mass obtained from these fits are collected in Table III. For illustration, we also show in the table the value of \bar{m}_{ud} obtained from a fit (denoted as L4 here and B in [9]) without logarithmic discretization terms, i.e., with $P_3 = P_6 = 0$ in Eq. (6), and without isospin breaking corrections in the FSEs.

For the strange quark mass we collect the results of the different fits in Table IV, where we use the short notation K-SU(2), K-SU(3), η_s -SU(2), and η_s -SU(3) for distinguishing the determinations from the kaon and η_s masses, and based on SU(2)- and SU(3)-ChPT.

The results for the ratio m_s/m_{ud} are given in Table V.

Finally, for the charm quark mass and the ratio m_c/m_s the results are collected in Tables VI and VII, where D , D_s , or η_c indicates the meson whose mass is used as input. These analyses are practically insensitive to the choice of the fit in the pion sector and only the results obtained from

TABLE III. Results for the up/down quark mass in the MS scheme at 2 GeV, as obtained from fits L1, L2, L3, and L4.

	L1	L2	L3	L4
\bar{m}_l [MeV]	3.55(14)	3.75(7)	3.78(17)	3.47(11)

TABLE IV. Results for the strange quark mass in the $\overline{\text{MS}}$ scheme at 2 GeV, as obtained from the different fits within the light and strange quark sectors.

\bar{m}_s [MeV]	K-SU(2)	K-SU(3)	η_s -SU(2)	η_s -SU(3)
L1	92.1(3.8)	94.7(2.2)	96.0(2.6)	95.5(2.1)
L2	91.6(3.9)	94.6(2.3)	95.4(2.6)	95.3(1.9)
L3	95.4(3.8)	94.7(2.1)	99.4(2.9)	97.7(2.2)

TABLE V. Results for the ratio m_s/m_{ud} , as obtained from the different fits within the light and strange quark sectors.

m_s/m_{ud}	K-SU(2)	K-SU(3)	η_s -SU(2)	η_s -SU(3)
L1	26.9(5)	27.2(5)	27.6(4)	27.3(7)
L2	27.1(5)	26.9(3)	27.5(3)	26.8(3)
L3	25.7(5)	26.0(6)	26.5(6)	26.0(7)

TABLE VI. Results for the charm quark mass in the $\overline{\text{MS}}$ scheme at 2 GeV, as obtained from the different fits within the charm sector.

	D	D_s	η_c
\bar{m}_c [GeV]	1.14(3)	1.14(3)	1.15(2)

TABLE VII. Results for the ratio m_c/m_s , as obtained from the different fits within the strange quark sector, and from the analysis of the D meson mass in the charm sector.

	K-SU(2)	K-SU(3)	η_s -SU(2)	η_s -SU(3)
m_c/m_s	12.4(4)	12.1(2)	11.9(2)	12.0(3)

the fit L1 are shown in the tables. Similarly, for the ratio m_c/m_s the values shown in Table VII correspond to the analysis of the D meson only, since the analyses of the D_s or η_c mesons yield practically identical results.

- [1] A. Bazavov *et al.*, *Rev. Mod. Phys.* **82**, 1349 (2010).
- [2] A. Bazavov *et al.* (MILC Collaboration), *Proc. Sci.*, CD09 (2009) 007.
- [3] C. Allton *et al.* (RBC-UKQCD Collaboration), *Phys. Rev. D* **78**, 114509 (2008).
- [4] S. Aoki *et al.* (PACS-CS Collaboration), *Phys. Rev. D* **81**, 074503 (2010).
- [5] C. T. H. Davies *et al.*, *Phys. Rev. Lett.* **104**, 132003 (2010).
- [6] I. Allison *et al.* (HPQCD Collaboration), *Phys. Rev. D* **78**, 054513 (2008).
- [7] M. Constantinou *et al.*, *J. High Energy Phys.* 08 (2010) 068.
- [8] E. E. Scholz, *Proc. Sci.*, LAT2009 (2009) 005.
- [9] R. Baron *et al.* (ETM Collaboration), *J. High Energy Phys.* 08 (2010) 097.
- [10] B. Blossier *et al.* (ETM Collaboration), *J. High Energy Phys.* 04 (2008) 020.
- [11] P. Weisz, *Nucl. Phys.* **B212**, 1 (1983).
- [12] R. Frezzotti, P. A. Grassi, S. Sint, and P. Weisz (Alpha Collaboration), *J. High Energy Phys.* 08 (2001) 058.
- [13] Ph. Boucaud *et al.* (ETM Collaboration), *Phys. Lett. B* **650**, 304 (2007).
- [14] Ph. Boucaud *et al.* (ETM Collaboration), *Comput. Phys. Commun.* **179**, 695 (2008).
- [15] C. Urbach (ETM Collaboration), *Proc. Sci.*, LAT2007 (2007) 022.
- [16] P. Dimopoulos, R. Frezzotti, G. Herdoiza, K. Jansen, C. Michael, and C. Urbach (ETM Collaboration), *Proc. Sci.*, LATTICE2008 (2008) 103.
- [17] R. Frezzotti and G. C. Rossi, *J. High Energy Phys.* 08 (2004) 007.
- [18] R. Frezzotti and G. C. Rossi, *J. High Energy Phys.* 10 (2004) 070.
- [19] A. M. Abdel-Rehim, R. Lewis, R. M. Woloshyn, and J. M. S. Wu, *Phys. Rev. D* **74**, 014507 (2006).
- [20] S. R. Sharpe and J. M. S. Wu, *Phys. Rev. D* **71**, 074501 (2005).
- [21] R. Frezzotti, G. Martinelli, M. Papinutto, and G. C. Rossi, *J. High Energy Phys.* 04 (2006) 038.
- [22] B. Jegerlehner, [arXiv:hep-lat/9612014](https://arxiv.org/abs/hep-lat/9612014).
- [23] K. Jansen, M. Papinutto, A. Shindler, C. Urbach, and I. Wetzorke (XLF Collaboration), *J. High Energy Phys.* 09 (2005) 071.
- [24] C. McNeile and C. Michael (UKQCD Collaboration), *Phys. Rev. D* **73**, 074506 (2006).
- [25] G. P. Lepage, B. Clark, C. T. H. Davies, K. Hornbostel, P. B. Mackenzie, C. Morningstar, and H. Trotter, *Nucl. Phys. B, Proc. Suppl.* **106-107**, 12 (2002).
- [26] R. Sommer, *Nucl. Phys.* **B411**, 839 (1994).
- [27] O. Bar, *Phys. Rev. D* **82**, 094505 (2010).
- [28] P. Dimopoulos, R. Frezzotti, C. Michael, G. C. Rossi, and C. Urbach, *Phys. Rev. D* **81**, 034509 (2010).
- [29] G. Colangelo, U. Wenger, and J. M. S. Wu, *Phys. Rev. D* **82**, 034502 (2010).
- [30] C. Aubin *et al.* (HPQCD Collaboration), *Phys. Rev. D* **70**, 031504 (2004).
- [31] K. G. Chetyrkin and A. Retey, *Nucl. Phys.* **B583**, 3 (2000).
- [32] A. Roessl, *Nucl. Phys.* **B555**, 507 (1999).
- [33] S. R. Sharpe, *Phys. Rev. D* **56**, 7052 (1997); **62**, 099901(E) (2000).
- [34] M. Constantinou *et al.* (ETM Collaboration), [arXiv:1009.5606](https://arxiv.org/abs/1009.5606).
- [35] B. Blossier *et al.*, *J. High Energy Phys.* 04 (2010) 049.
- [36] K. G. Chetyrkin, J. H. Kuhn, A. Maier, P. Maierhofer, P. Marquard, M. Steinhauser, and C. Sturm, *Phys. Rev. D* **80**, 074010 (2009).
- [37] R. Baron *et al.*, *J. High Energy Phys.* 06 (2010) 111.
- [38] R. Baron *et al.* (ETM Collaboration), *Comput. Phys. Commun.* **182**, 299 (2011).